Aquatic Sciences (2021) 83:23
https://doi.org/10.1007/s00027-021-00778-8

Aquatic Sciences

RESEARCH ARTICLE

Export of photolabile and photoprimable dissolved organic carbon from the Connecticut River

Byungman Yoon[1,4] · Jacob D. Hosen[1] · Ethan D. Kyzivat[1,5] · Jennifer H. Fair[1,3] · Lisa C. Weber[1] · Kelly S. Aho[1] · Rachel Lowenthal[1] · Serena Matt[1] · William V. Sobczak[2] · Jamie B. Shanley[3] · Jon Morrison[3] · James E. Saiers[1] · Aron Stubbins[4] · Peter A. Raymond[1]

Received: 23 June 2020 / Accepted: 12 January 2021

Abstract

Dissolved organic carbon (DOC) impacts water quality, the carbon cycle, and the ecology of aquatic systems. Understanding what controls DOC is therefore critical for improving large-scale models and best management practices for aquatic ecosystems. The two main processes of DOC transformation and removal, photochemical and microbial DOC degradation, work in tandem to modify and remineralize DOC within natural waters. Here, we examined both the photo- and microbial remineralization of DOC (photolability and biolability), and the indirect phototransformation of DOC into biolabile DOC (photoprimed biolability) for samples that capture the spatiotemporal and hydrological gradients of the Connecticut River watershed. The majority of DOC exported from this temperate watershed was photolabile and the concentration of photolabile DOC correlated with UV absorbance at 254 nm ($r^2 = 0.86$). Phototransformation of DOC also increased biolability, and the total photolabile DOC (sum of photolabile and photoprimed biolabile DOC) showed a stronger correlation with UV absorbance at 254 nm ($r^2 = 0.92$). We estimate that as much as 49% (SD = 3.3%) and 10% (SD = 1.1%) of annual DOC export from the Connecticut River is directly photolabile and photoprimable, respectively. Thus, 2.82 Gg C year^{-1} (SD = 0.67 Gg C year^{-1}) or 1.13 Mg C km^{-2} year^{-1} (SD = 0.27 km^{-2} year^{-1}) of total photolabile DOC escapes photochemical degradation within the river network to be exported from the Connecticut River each year.

Keywords DOC · Photolability · Photopriming

Introduction

Dissolved organic carbon (DOC) is a master variable, referred to as "the great modulator" (Prairie 2008) of aquatic systems. As the largest pool of organic carbon in inland waters (Fisher and Likens 1973; McDowell and Likens 1988), DOC affects numerous ecosystem processes such as primary production, microbial metabolism, community structure, pH, heat budgets, thermal stratification, light availability, and drinking water quality (Christman et al. 1983; Carpenter et al. 1998; Kitis et al. 2001; Kirchman et al. 2004; Judd et al. 2006; Caplanne and Laurion 2008; Erlandsson et al. 2010). Concurrent with the advances made on the conceptual frameworks for studying DOC in inland waters (Vannote et al. 1980, Junk et al. 1989, Thorp and Delong 1994, Raymond et al. 2016), studies in recent decades have also demonstrated that DOC processes have implications beyond watershed boundaries. For example, the quantity and quality of DOC are now identified as key drivers of CO_2

Supplementary Information The online version contains supplementary material available at https://doi.org/10.1007/s00027-021-00778-8.

✉ Byungman Yoon
b.yoon@northeastern.edu

1 School of the Environment, Yale University, New Haven, CT, USA

2 Biology Department, College of the Holy Cross, Worcester, MA, USA

3 New England Water Science Center, U.S. Geological Survey, Reston, USA

4 Department of Marine and Environmental Sciences, Civil and Environmental Engineering, and Chemistry and Chemical Biology, Northeastern University, Boston, MA, USA

5 Department of Earth, Environmental and Planetary Science, Brown University, Providence, RI, USA

Published online: 09 February 2021

emission to the atmosphere from inland waters (Raymond et al. 2013; Hotchkiss et al. 2015) and coastal margins (Cai 2011; Fichot and Benner 2014). Therefore, advancing our understanding of how DOC is transported and modified is a goal shared across several disciplines.

Photochemical processes driven by sunlight are one of the main mechanisms that regulate the removal and compositional change of DOC (Mopper et al. 2015). Sunlight availability partly determines how much DOC can be mineralized to CO_2 (Miller and Zepp 1995; Bertilsson and Tranvik 2000), utilized by microbes (Lindell et al. 1995), and transported downstream. The colored, aromatic component of DOC is modified by photochemical reactions in natural waters (Mopper et al. 2015). As these colored compounds absorb the photochemically active radiation, they are preferentially photodegraded, altering the composition of DOC remaining for downstream transport (Stubbins et al. 2010). DOC phototransformation also alters the fraction of DOC susceptible to microbial uptake (i.e., DOC biolability; Lindell et al. 1995; Moran and Zepp 1997; Tranvik and Bertilsson 2001; Fellman et al. 2013; Cory et al. 2014; Bittar et al. 2015; Ward et al. 2017; Cory and Kling 2018). First presented as "priming" by Strome and Miller (1978), and also referred to as "photo-bio" degradation or photostimulated bacterial respiration (Cory et al. 2014; Cory and Kling 2018), the photoalteration of aromatic-rich DOC generally increases DOC biolability (Moran and Zepp 1997). Photodegradation preferentially removes aromatics, leaving behind a DOC pool enriched in aliphatics (Stubbins et al. 2010) and low molecular weight compounds (Mopper et al. 1991). Aliphatics and low molecular weight compounds are known to be more biolabile than bulk or aromatic DOC (Spencer et al. 2015; Berggren et al. 2010). In addition, aromatic compounds can inhibit enzymatic activities and microbial utilization of DOC (Mann et al. 2014). Thus, photopriming may result from both the increase of biolabile DOC and the alleviation of microbial inhibition by aromatics. In some cases, sunlight can reduce the availability of biolabile DOC. For instance, when highly biolabile DOC of low aromatic content from cyanobacteria is photodegraded there can be a net photo-removal of biolabile DOC resulting in negative photopriming (Bittar et al. 2015). Thus, initial DOC quality influences the way in which sunlight modifies DOC biolability. To date, the variability of photolability and photoprimed biolability across large spatiotemporal and hydrological scales have not been assessed within a single, methodologically consistent study.

The rate of photochemical DOC processing is primarily governed by three factors: availability of sunlight reaching the water surface; competition for light in the water column; and the efficiency at which DOC is degraded once light is absorbed (Cory and Kling 2018). Physical and environmental factors such as latitude, season, canopy cover, and cloud cover affect the level of light reaching the surface, and suspended sediments and other light absorbing or scattering substances in the water column can further affect the proportion of light absorbed by chromophoric dissolved organic matter (CDOM; Juday and Birge 1933; Osburn et al. 2009). The residence time of DOC within the photic zone during transport through an ecosystem can also influence the degree of DOC processing (Vähätalo and Wetzel 2008; Catalán et al. 2016). Ranging from a few days to multiple years, the wide range of residence times across inland water networks influences how much DOC can be photomineralized, microbially utilized, or transported out to the coastal margin. Furthermore, recent studies show storm events play a central role in controlling DOC fluxes (Raymond and Saiers 2010; Vidon et al. 2018). Shortened residence time (Sayama and McDonell 2009), increase in suspended solids (Benda and Dunne 1997), change in DOC source, concentration and chemistry (Fellman et al. 2009; Yoon and Raymond 2012; Wilson et al. 2013; Vidon et al. 2018; Wagner et al. 2019), and decrease in light availability (Jennings et al. 2012) are all common features of storm events. Thus, changes during storm events affect amount of the DOC entering waters, the chemistry and photoreactivity of DOC entering waters, the rate of DOC photochemical processes in the water, and the amount of time for photoreactions to occur.

Numerous studies have identified CDOM with aromatic moieties as the major light absorbing chromophores and reported positive relationship between CDOM and photomineralization (Mopper et al. 2015; Osburn et al. 2009; Lapierre et al. 2013; Lapierre and del Giorgio 2014; Koehler et al. 2016; Ward and Cory 2016). However, most recent studies on photopriming have focused on specific ecosystems (e.g. alpine streams, boreal/arctic lakes) and on short timescales (Tranvik and Bertilsson 2001; Fasching and Battin 2012; Cory et al. 2014; Ward et al. 2017). Thus, our knowledge on the prevalence and variability of photopriming is limited to select ecosystems and specific seasons. Furthermore, there is no established method to assess the concentration of photoprimable biolabile DOC at a high temporal resolution despite recent progress in continuous measurement of DOC quantity and quality via optical sensors (Downing et al. 2012; Pellerin et al. 2012; Shultz et al. 2018). This limitation is further exacerbated by the fact that most past lability studies are not intercomparable due to different experimental designs (McDowell et al. 2006). Limited representation of both spatial and temporal variation among past studies, the lack of a convenient model based on optical data, and the difficulty in combining the results of past studies all hinder the assessment of when and where the photoreactive DOC fluxes are exported at large spatiotemporal scale.

To address this knowledge gap, we present models based on optical indices that can estimate photolabile and photoprimed biolabile DOC for a wide range of DOC

concentration and composition. We assessed biolability, photolability, and photoprimed biolabilty of samples collected from 50 different sites over a 2-year period in temperate New England. The number of sites and duration of the study enabled the collection of water samples spanning a wide range of land covers, seasons, hydrological conditions, and temperatures. This diverse suite of samples was submitted to a uniform set of biological, photochemical, and coupled biological and photochemical incubation experiments. The resulting data characterize the potential lability of DOC under uniform experimental conditions, which enabled elucidation of the intrinsic lability of DOC across a multitude of samples. By coupling data from these lability experiments with DOC optical data, a simple optical proxy for photolabile including photoprimed biolabile DOC was developed and used to estimate the export of photolabile DOC from the Connecticut River over a 5-year period. The estimates reveal both the quantity and timing of the photolabile flux leaving the riverine network, and highlight the importance of hydrological control on the dynamics of DOC export.

Methods

Site description and sampling

The Connecticut River is the longest (mainstem length = 660 km) and the largest (watershed area = 29,000 km^2) river in the New England region of the US with an annual mean temperature from − 1.7 °C in the north to 10.9 °C in the south, where it drains to Long Island Sound (PRISM Climate Group; Fig. 1; Supplementary Fig. S1). The moderate size, temperature gradient, and the network of longstanding US Geological Survey (USGS) gauging stations make the Connecticut River a near-ideal study watershed (Fig. 1). Samples were collected during 2015–2017 from 50 sites that encompass a range of the land cover composition (Homer et al. 2015) and watershed sizes (Fig. 1; Supplementary Fig. S1; Supplementary Table S1). Two tributaries, the Farmington River in Connecticut and Passumpsic River in Vermont, were selected for nested sampling where streams in small to larger watersheds within the river basins were sampled with automatic samplers (ISCO Avalanche) to assess DOC quality through the river network, especially during hydrologic events (Fig. 1, Supplementary Fig. S2). Other major 4th and 5th order tributaries (EPA National Hydrography Dataset Plus Version 2) of the Connecticut River were sampled during hydrologically important periods (e.g., snowmelt, drought, and storms) over the two years. Thus, samples captured event-driven, seasonal, and landscape related variation in DOC composition. Grab samples were filtered on site through 0.2 µm filters (Polyethersulfone;

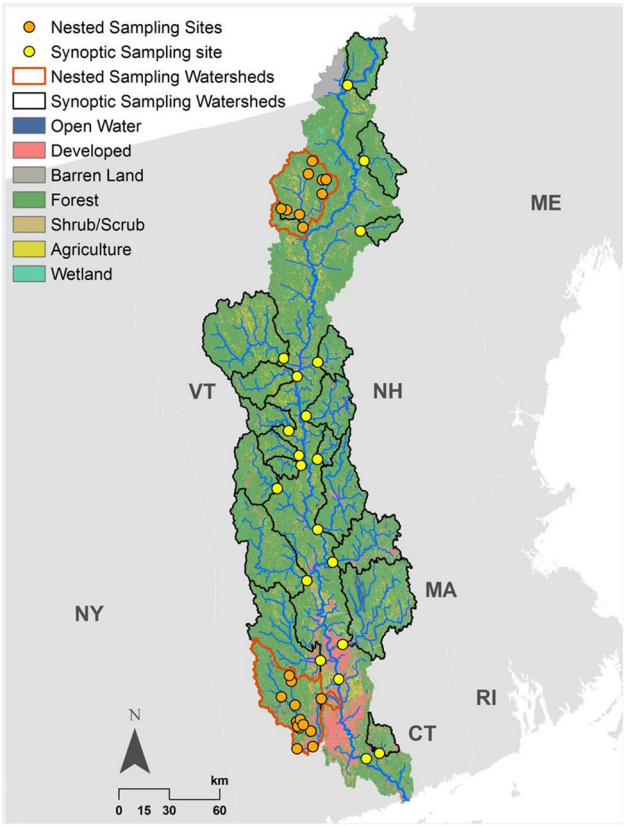

Fig. 1 The Connecticut River watershed and sampling sites. Nested sites were sampled at least biweekly and more frequently during storm events (every 3–6 h). Synoptic sites were sampled during hydrologically important periods (e.g., snowmelt, drought, and storms). The background layer shows the land cover of the watershed (Homer et al. 2015). See Supplementary Table S1 for detailed description of the watershed size and land cover composition. Watershed area and boundaries were derived from National Hydrography Dataset (USGS NHD) in ArcGIS (Esri)

Waterra USA Inc.) with a peristaltic pump, immediately refrigerated, and returned to the laboratory. Samples from autosamplers were refrigerated within the autosampler at 3 °C until retrieval and were filtered (0.2 µm) within 3 days of collection at Yale University or USGS station (Montpelier, Vermont). Discharge data was obtained from USGS (USGS Water Data for the Nation).

Dissolved organic carbon analysis

DOC concentration was measured as non-purgeable organic carbon concentration with a Shimadzu Total Organic Carbon Analyzer (Kyoto, Japan), and was quality checked with third party references (Ultra Scientific Standards, Santa Clara, USA). Ultraviolet–visible absorbance was measured using a Horiba Aqualog (Kyoto, Japan) with MilliQ ultrapure water as blank, and zero offset at 650–700 nm range. Absorbance

reported by the instrument was converted to decadic absorption coefficients at 254 and 412 nm (a_{254} and a_{412}):

$$a_\lambda = \frac{A_\lambda}{l} \quad (1)$$

where A_λ is absorbance,λ is wavelength (nm), and l is pathlength of the quartz cuvette in meters. To assess aromaticity of samples, we calculated Specific UV Absorbance at 254 nm (SUVA in L mg C^{-1} m^{-1}) as the decadic absorbance at 254 nm normalized by DOC concentration (Weishaar et al. 2003). Spectral slope (S) was calculated by fitting the absorbance data to

$$a_\lambda = a_{\lambda \mathrm{ref}} e^{-S(\lambda - \lambda_{\mathrm{ref}})} \quad (2)$$

where a is Napierian absorption coefficient (m^{-1}) and λ_{ref} is reference wavelength (Twardowski et al. 2004). Spectral Slope Ratio (S_R) was calculated as the ratio between $S_{275\text{-}295}$ and $S_{350\text{-}400}$ (in nm^{-1}; Helms et al. 2008). DOC concentration and optical properties were measured within 10 days of collection.

DOC lability and priming measurement

We performed three types of common laboratory lability experiments: biolability, photolability, and photoprimed biolability (Fig. 2). The lability tests conducted for this study have been employed extensively in peer-reviewed studies and provide an estimate for the proportion of DOC that has the potential to be lost via biological or photochemical processes under the experimental conditions rather than quantifying the in-situ DOC loss or the absolute lability of DOC under natural conditions (See Supplementary Tables S2-3 for a list of past lability studies and their methods). Although both biolability and photolability experiments spanned the same timeframe in the laboratory (30 days), they were not designed for comparison between relative photolability and biolabilty. Instead, these experiments were designed to allow biolability and photolability to be independently compared across samples within each experiment.

Biolability

Biolability was measured through 30-day, room-temperature (~22 °C), dark incubations where native raw water inoculum (1% by volume) and nutrient amendment solution (1 mL) were added to filtered samples (125 mL; n = 461; Fig. 2; Supplementary Method S1). Our study incorporated nutrient amendment of nitrogen (as both ammonium and nitrate) and phosphorous (as phosphate) so that DOC biolability could be tested without nutrient limitation. Nutrient amendments raised nitrogen concentration by 70 Mμ (as ammonium and nitrate) and phosphate concentration by 10 µM resulting in C:N and C:P ratios below the Redfield ratio (Redfield 1934) for typical Connecticut River samples with DOC concentration up to ~ 10 mg C L^{-1}. The samples were filtered again through 0.2 µm at the end of the 30-day incubation period prior to analysis. Blanks and quality control tests under the same protocol confirmed that the addition of raw inoculum and nutrient solution had negligible effect on

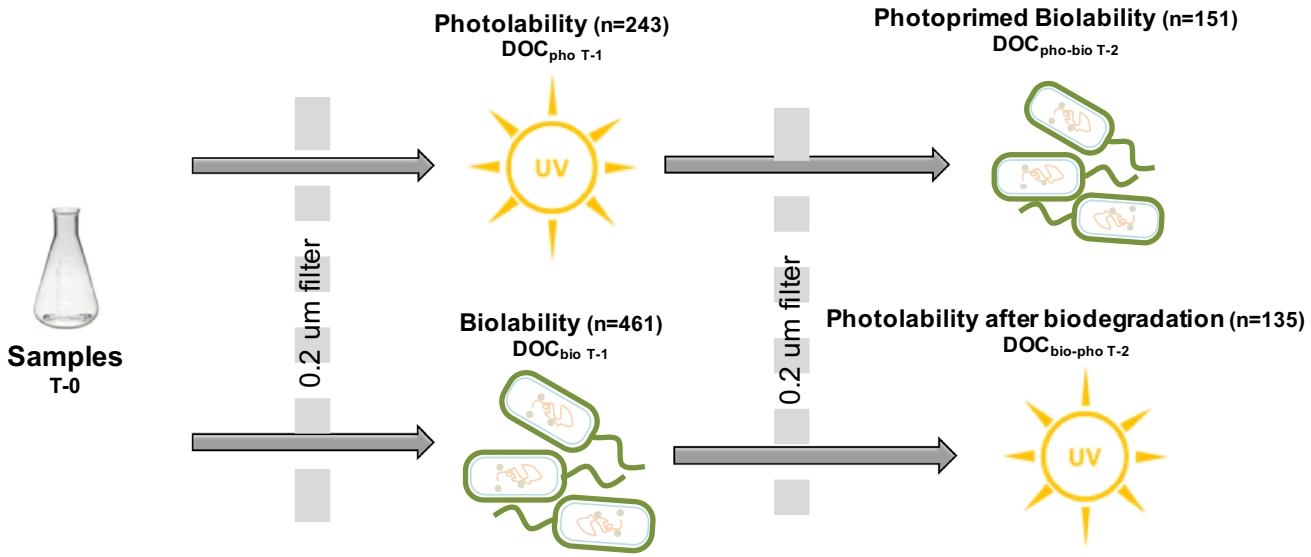

Fig. 2 Experimental design for lability and priming tests. Photolabile and biolabile dissolved organic carbon (DOC) concentrations were calculated as DOC loss during 30-day incubations. Photoprimed biolabile DOC concentration is calculated as DOC loss during bioassay test following a 30-day photolability test, minus the loss occurred during the biolability test. Percent lability terms are calculated as DOC loss normalized by the initial DOC concentration

DOC concentration or absorbance. Further, the use of native inoculum in our method ensured that the effect of inoculum addition is consistently minimal across all samples. The methods applied here do not distinguish between flocculation and microbial utilization. Biolabile DOC concentration and % biolability were calculated as

$$\text{Biolabile DOC concentration} = \left[\text{DOC}_{\text{T}-0}\right] - \left[\text{DOC}_{\text{bio T}-1}\right] \quad (3)$$

$$\text{Biolability (\%)} = \left(\left[\text{DOC}_{\text{T}-0}\right] - \left[\text{DOC}_{\text{bio T}-1}\right]\right) / \left[\text{DOC}_{\text{T}-0}\right] \times 100 \quad (4)$$

where $[\text{DOC}_{\text{T-0}}]$ and $[\text{DOC}_{\text{bio T-1}}]$ are the concentration of DOC at the onset and the end of incubation, respectively. It should be noted that biodegradation of DOC during the bioassay would occur predominantly in the water column by free living bacteria or at the bottle's surface via attached bacteria, which are introduced through a small volume of inoculum. In comparison, natural riverine systems have abundant bacteria throughout the water column, riverbank, streambed, and hyporheic surfaces. This implies that the natural environment has the potential to not only speed rates of biodegradation but also to increase the total amount of DOC that is identified as biolabile in comparison to the bioassay.

Photolability

Photolability was measured through 30-day simulated solar irradiation inside a custom-made photochamber (n = 243; Fig. 2; Stubbins et al. 2017). The photochamber was constructed using 10 UV-light bulbs (10 × QUV-340 bulbs, Q-Lab Corporation) that emit broadband irradiance that closely matches the spectral shape and flux of natural sunlight across 295–365 nm, the main wavelength range for environmental photochemical reactions involving CDOM (Mopper et al. 2015). The integrated irradiance from the bulbs is ~ 14.4 ± 0.7 W m^{-2} (Stubbins et al. 2017) or ~ 1.24 ± 0.06 MJ m^{-2} day^{-1}, which is similar to the mean daily irradiance during summer months in the Connecticut River watershed (1.16 ± 0.51 MJ m^{-2} day^{-1} across 295–400 nm). The mean irradiance for the watershed was calculated by multiplying the ratio of solar irradiance in 295–400 nm to 400–1110 nm in Simple Model for Atmospheric Transmission of Sunshine (SMARTS2, Gueymard 2001) with long-term solar radiation data collected at the Harvard Forest (daily total irradiance across 400–1100 nm in July and August during 2001–2016 period; Harvard Forest Data Archive). The photolability incubation was conducted with 0.2 µm filtered water samples in custom-made 120 mL cylindrical quartz tubes (diameter 3 cm, length 15 cm) with 10–15 mL of headspace. Quartz test tubes containing the samples were horizontally placed 20 cm below the light source, and the tubes were repositioned after 15 days to promote even irradiance across the samples. The samples were filtered at the end of the test period. The effective pathlength of these tubes is significantly shorter than the depth of water in even small streams, not to mention the larger rivers sampled here. Thus, absolute amounts of photolabile DOC quantified in these experiments for 30 days would take longer than 30 days to realize in the field. The methods applied here do not distinguish between flocculation and photolability. Photolabile DOC concentration and % photolability were calculated as

$$\text{Photolabile DOC concentration} = \left[\text{DOC}_{\text{T}-0}\right] - \left[\text{DOC}_{\text{pho T}-1}\right] \quad (5)$$

$$\text{Photolability (\%)} = \left(\left[\text{DOC}_{\text{T}-0}\right] - \left[\text{DOC}_{\text{pho T}-1}\right]\right) / \left[\text{DOC}_{\text{T}-0}\right] \times 100 \quad (6)$$

where $[\text{DOC}_{\text{T-0}}]$ and $[\text{DOC}_{\text{pho T-1}}]$ are the concentration of DOC at the beginning and the end of the irradiance exposure, respectively.

Photoprimed biolability

To assess photoprimed biolability, a subset of the irradiated samples were subsequently re-filtered, inoculated with native bacteria, nutrient amended, and incubated in the dark for 30-days to quantify the effect of photochemical degradation on DOC biolability (n = 151; Fig. 2). Photoprimed biolabile DOC concentration and % photoprimed biolability were calculated as:

$$\text{Photoprimed Biolabile DOC Concentration} = \left[\text{DOC}_{\text{pho T}-1}\right] - \left[\text{DOC}_{\text{pho}-\text{bio T}-2}\right] - \left[\text{DOC}_{\text{bio T}-1}\right] \quad (7)$$

$$\text{Photoprimed Biolability (\%)} = \left(\left[\text{DOC}_{\text{pho T}-1}\right] - \left[\text{DOC}_{\text{pho}-\text{bio T}-2}\right] - \left[\text{DOC}_{\text{bio T}-1}\right]\right) / \left[\text{DOC}_{\text{T}-0}\right] \times 100 \quad (8)$$

where $[DOC_{pho\ T-1}]$, $[DOC_{pho-bio\ T-2}]$, $[DOC_{bio\ T-1}]$, and $[DOC_{T-0}]$ are the DOC concentrations of samples at the end of 30-day photolability test, at the end of 30-day bioincubation following the photolabilty test, at the end of 30-day biolability test, and before the initial photolability test, respectively. The resulting % photoprimed biolability is directly comparable to % biolability because both are normalized by the initial concentration (Supplementary Method S2). All samples were filtered at 0.2 µm at the end of each incubation period. For quantifying the effect of photopriming and also for comparison across different samples, we calculated the ratio of photoprimed biolabile DOC concentration to biolabile DOC concentration. The sum of photolabile and photoprimed biolabile DOC is referred to as total photolabile DOC from hereon.

Effect of biodegradation on predicting photolability

In addition to the three lability experiments above, a subset of samples that had been through the biolability tests were subjected to photolability tests (n = 135; Fig. 2). This secondary photolability test aimed to examine how biological degradation of the DOC pool affects the efficacy of predictor variables for photolability. Photolabile DOC loss after biodegradation was calculated as:

$$\text{Photolabile DOC loss after Biodegradation} = [DOC_{bio\ T-1}] - [DOC_{bio-pho\ T-2}] \quad (9)$$

where $[DOC_{bio\ T-1}]$ and $[DOC_{bio-pho\ T-2}]$ denote the DOC concentration at the end of biolability test and at the end of subsequent photolability test, respectively.

Statistical analysis

Photolabile and total photolabile DOC concentrations were modeled with a254 and a412 using linear regression. Confidence intervals for the models were estimated with nonparametric bootstrapping (95% confidence interval, 1000 replications) with boot package (Canty and Ripley 2020; Davison and Hinkley 1997) in R (R Core Team 2013). The choice of method for calculating the confidence intervals (e.g. first order normal approximation, Hall's method, percentile, Studentized) did not affect the outcome and the result of first order normal approximation is shown here (Fig. 6, Supplementary Fig. S9, Supplementary Result S1). The linear models were used in conjunction with historic USGS absorbance data to estimate the flux of the photolabile and total photolabile DOC leaving the Connecticut River through LOAD ESTimator (LOADEST; Runkel et al. 2004). LOADEST calculates daily, monthly, and yearly loads of a constituent across specific time periods by building a regression between the load and discharge. A sampling site located in Thompsonville, Connecticut (USGS Station 0118400) was chosen as the reference site for the Connecticut River as it is the furthest downstream gauging station on the main stem of the river unaffected by tides and also a site with historic USGS data for both DOC concentration and a254. To calculate the photolability and total photolability of the Connecticut River DOC flux, we first estimated the flux of DOC leaving the Connecticut River at Thompsonville with samples from this study (n = 44) and the USGS record (n = 172). Then, we repeated the same procedure with all available a254 data (41 from this study and 79 from USGS) and the two DOC models from this study to calculate the amount of photolabile DOC and total photolabile DOC flux. All flux calculations were based on adjusted maximum likelihood estimation (AMLE) values from LOADEST.

Changes in DOC concentration that were below the analytical limit of quantification (~ 0.2 mg C L^{-1}) were converted to 0. This procedure corrected two negative and one positive biolability values observed during our experiment, resulting in three samples that recorded 0% biolability. We report coefficient of determination (r^2) from linear regressions and Welch's t-test p-values where applicable.

Results

Environmental and DOC variability captured across samples

The samples in this study captured a wide range of environmental conditions, DOC concentration, and DOC quality. The samples were collected across all seasons over two years from nested watersheds of varying sizes (0.4 km^2 to 28,200 km^2; Fig. 1; Supplementary Table S1) and across a wide range of surface temperature (mean annual temperature from −1.7 to 10.9 °C; Supplementary Fig. S1). Water temperature during the sampling period ranged from 0 to 29 °C. Area-normalized discharge at sampling ranged from 0.005 cm day^{-1} during winter freeze to 4.97 cm day^{-1} during storm events representing 0.05–99.7% exceedance values observed across the sampling sites since 1987 (Supplementary Fig. S2). Thus, the samples represent the near-entirety of hydrological conditions and temperature range observed across our sites in the Connecticut River.

The DOC concentration and quality captured in the sample collection also represent large and ecologically relevant ranges (Figs. 3, 4, 5; Supplementary Figures S3 and S5; Supplementary Table S4). DOC concentration of the initial, field samples ranged from < 0.5 mg C L^{-1} to 19.1 mg C L^{-1}, decadic absorbance coefficient at 254 nm (a254) from 0.4 to 67.9 m^{-1}, decadic absorbance coefficient at 412 nm (a412) from 0.0 to 5.7 m^{-1} and SUVA from 0.21 to 6.2 L mg C^{-1} m^{-1}. $S_{275-295}$ ranged from 0.011 to 0.027 nm^{-1}, $S_{350-400}$

from 0.014 to 0.031 nm^{-1}, and the Spectral Slope Ratio (S_R) from 0.35 to 1.92 (Supplementary Figure S3). The range of DOC concentration and SUVA values presented in the samples cover the average values found across major rivers in the continental US (Spencer et al. 2012), suggesting results from this study are relevant to a diversity of inland waters. The SUVA values of the samples, in particular, provide a wide range that has not been tested under a single, methodologically consistent lability study.

Biolability

DOC biolability (%) ranged from 0 to 77.6% (Figs. 3a, 4a) with a mean of 15.6% (n = 461, SD = 11.3%). Most of the samples showed a decrease in CDOM absorbance after the biolability assay (> 95% of samples at a254 nm and > 90% for a412 nm), and their average CDOM loss was 15.0% (SD = 20.0%; Welch Two sample t-test, $p < 0.01$) and 18.7% (SD = 23.7%; $p < 0.01$) for a254 and a412, respectively. SUVA increased by 1.5% on average (SD = 30.1%; $p > 0.05$). Average $S_{275\text{-}295}$ and $S_{350\text{-}400}$ changes were − 1.4% (SD = 8.9%; $p > 0.5$) and 5.2% (SD = 10.2%; $p < 0.001$), respectively, which in turn resulted in 5.6% decrease in average S_R (SD = 11.1%; $p < 0.001$). Changes in absorbance after bioincubation ranged from − 98.5 to 83.1% for a254 and − 98.2 to 110.2% for a412 nm. Biolabile DOC concentration showed a weak linear correlation with bulk DOC concentration ($r^2 = 0.24$, $p < 0.001$; Fig. 3). Linear correlations between optical properties and % biolability were tested. SUVA was the best predictor for percent biolability

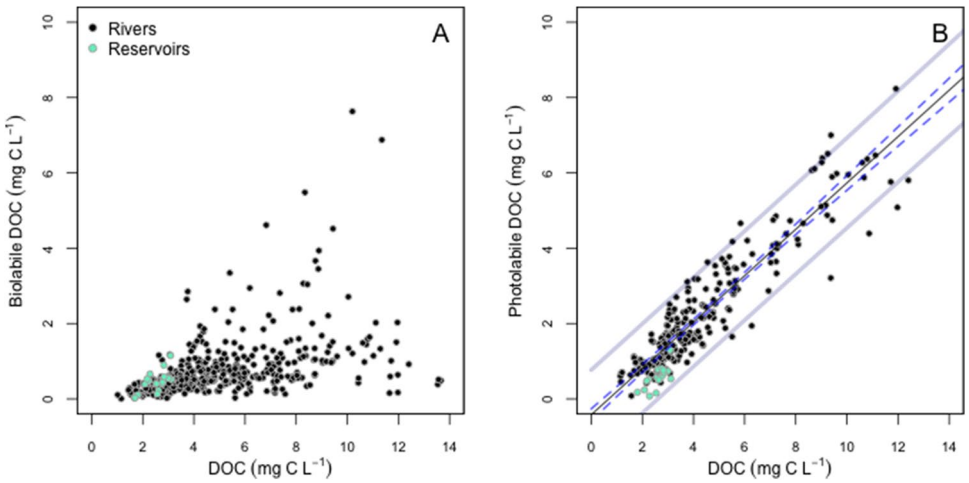

Fig. 3 Bulk dissolved organic carbon (DOC) concentration versus **a** biolabile DOC concentration and **b** photolabile DOC concentration (Slope = 0.615 ± 0.016, intercept = -0.421 ± 0.080, $r^2 = 0.86$, $p < 0.001$). Solid black, dashed blue, and light blue lines respectively represent regression, confidence intervals (95%), and prediction intervals (95%)

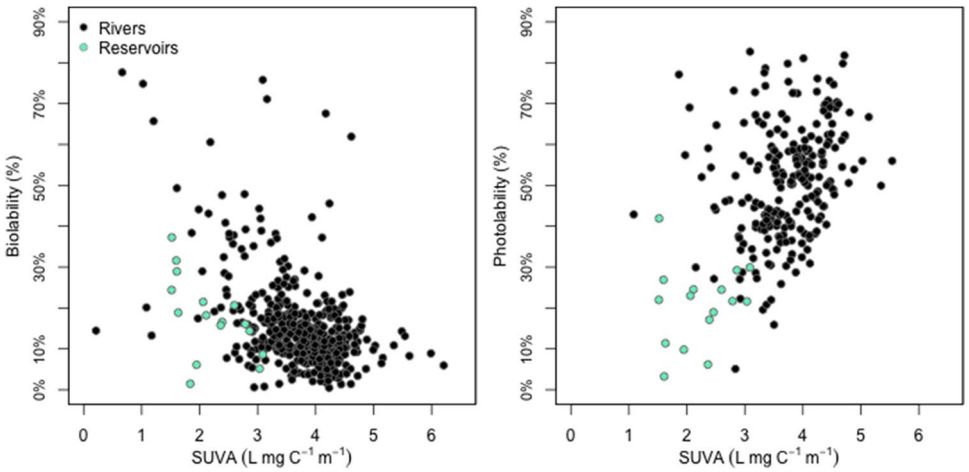

Fig. 4 Specific UV Absorbance at 254 nm (SUVA) versus **a** % biolability and **b** % photolability

($r^2 = 0.23$, $p < 0.001$; Fig. 4a). Neither percent nor concentration of biolabile DOC correlated significantly with watershed area, land cover composition, and area-normalized discharge (linear regressions, $r^2 < 0.1$, $p > 0.2$; Supplementary Figure S8).

Photolability

Photolabile DOC loss after 30-day incubations ranged from 0.07 to 8.2 mg C L^{-1} (Fig. 3b). CDOM a254 loss ranged from 48.1 to 100% (mean = 91.8%, SD = 6.8%; *p* value < 0.05; Supplementary Fig. S4A) and a412 loss ranged from 10.4 to 100% (mean = 96.4%, SD = 9.4%; p-value < 0.05; Supplementary Fig. S4B). SUVA decrease ranged from 3.7 to 100% (mean = 84.4%, SD = 10.4%; p value < 0.05), and the average SUVA at the end of irradiation was 0.54 L mg C^{-1} m^{-1} (SD = 0.34 mg C^{-1} m^{-1}). DOC % photolability ranged from 3.3 to 82.7% with a mean of 49.0% (n = 243, SD = 15.7%) and was positively correlated with SUVA and $S_{275\text{-}295}$, and negatively correlated with S_R (Fig. 4b; $r^2 = 0.20$, 0.31, and 0.30 for SUVA, $S_{275\text{-}295}$, and S_R, respectively, p values < 0.05). $S_{350\text{-}400}$, on the other hand, showed a weaker correlation with % DOC photolability ($r^2 = 0.11$, p value < 0.05). Photolabile DOC concentration correlated with a254 ($r^2 = 0.85$, p value < 0.05; Fig. 5a, Supplementary Result S1), a412 ($r^2 = 0.82$, p value < 0.05; Supplementary Fig. S5A, Supplementary Result S1), and bulk DOC concentration ($r^2 = 0.86$, p-value < 0.05; Fig. 3b). Photolability (%) of reservoir samples was significantly lower than the rest of the samples (Fig. 3b; mean % photolability = 20.8%, SD = 9.7%, n = 16; $p < 0.01$), and partly contributed to the higher variability of photolability observed in the lower DOC concentration range. Watershed area, land cover composition, and area-normalized discharge showed no significant correlation with % photolability ($r^2 < 0.1$, $p > 0.05$; Supplementary Figure S8).

Photoprimed biolability

Photoprimed biolabile DOC concentration ranged from −2.4 to 4.1 mg C L^{-1} (n = 151, mean = 0.75 mg C L^{-1}, SD = 1.1 mg C L^{-1}; 14.4% of the initial DOC, SD = 15.4%), and was greater than initial biolabile DOC concentration among 61.6% of tested samples (Supplementary Method S2). The average ratio of photoprimed to biolabile DOC concentration, an index for quantifying the strength of photopriming, was 2.4 (SD = 4.0). Concentration of photoprimed biolabile DOC linearly correlated with initial DOC concentration ($r^2 = 0.63$, p value < 0.05), a254 ($r^2 = 0.59$, p-value < 0.05), and a412 ($r^2 = 0.50$, p value < 0.05). Despite sharing the same set of predictors, photoprimed biolabile DOC and photolabile DOC concentrations showed a weak correlation ($r^2 = 0.05$). However, the ratio of photoprimed biolabile DOC to photolabile DOC was negatively correlated to residuals of the linear regression for photolabile DOC concentration versus a254 ($r^2 = 0.46$, p value < 0.05; Supplementary Fig. S6). That is, the samples that contained lower amounts of photolabile DOC than expected from our model resulted in greater production of photoprimed biolabile DOC. The sum of photolabile and photoprimed biolabile DOC concentration, which we term total photolabile DOC, showed strong linear correlation with a254 and a412

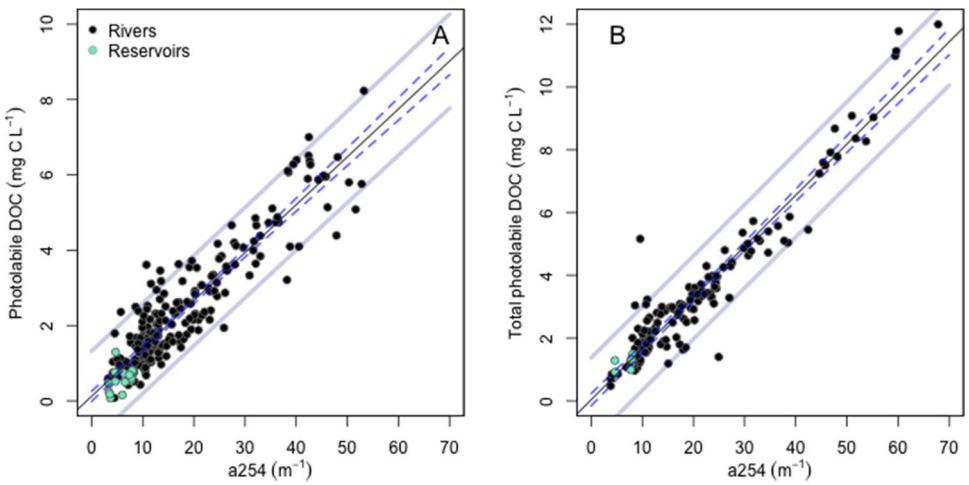

Fig. 5 Decadic absorption coefficient at 254 nm versus **a** photolabile dissolved organic carbon (DOC) concentration (Slope = 0.127 ± 0.003, intercept = 0.123 ± 0.068, $r^2 = 0.85$, $p < 0.001$) and **b** total photolabile DOC (photolabile DOC + photoprimed biolabile DOC; slope = 0.163 ± 0.004, intercept = 0.039 ± 0.099, $r^2 = 0.92$, $p < 0.001$). Solid black, dashed blank, and blue lines respectively represent regression, confidence intervals (95%), and prediction intervals (95%). See Supplementary Result S1 for bootstrap confidence intervals

(Fig. 5b, $r^2 = 0.92$; Supplementary Fig. S5B, $r^2 = 0.81$; See Supplementary Result 1 for bootstrap confidence interval). Total photolabile DOC ranged from 0.48 to 12.0 mg C L^{-1} (mean = 3.3 mg C L^{-1}, SD = 2.3 mg C L^{-1}; mean photolability = 60.7%, SD = 12.6% of the initial DOC).

Bioprimed photolability

Photolabile DOC concentrations after 30-day bioassays showed similar correlations with a254 as the initial, non-biodegraded samples (Supplementary Fig. S7). The biotreatment had no effect on the slope ($p > 0.5$) but affected the intercept of the regression between a254 and photolabile DOC concentration ($p < 0.001$; ANCOVA, Type II sum of squares). However, a regression model built with both sets of samples captured more than 97% of the variation seen across the two treatments (Supplementary Figure S7; Supplementary Result S2).

Photolabile DOC flux from the Connecticut River

Using the correlation between photolabile DOC concentration and a254 (Fig. 5), and available historic measurements of a254 for the Connecticut River mainstem, we were able to estimate the flux of photolabile and total photolabile DOC with LOADEST (Supplementary Result S2, Supplementary Figure S9). We estimate that approximately 49% (SD = 3.3%) of the annual DOC flux leaving the Connecticut River watershed was directly photolabile for the 2012–2016 period (at USGS gauging station 0118400 Thompsonville; furthest station on the mainstem of the river not affected by tides). When photoprimed biolabile DOC is included, 59% (SD = 4.3%) of the DOC flux was labile (Fig. 6). Per unit area, this translates to DOC load of 2.82 Gg C $year^{-1}$ (SD = 0.67 Gg C $year^{-1}$) or yield of 1.13 Mg C km^{-2} $year^{-1}$ (SD = 0.27 km^{-2} $year^{-1}$) that is not being mineralized during transport but is potentially susceptible to further degradation after delivery to Long Island Sound. The mean absolute error for the modeled photolability was −0.9%, and 6.8% of the predicted values had error greater than 10%. The LOADEST models did not show any biases across the hydrological gradient.

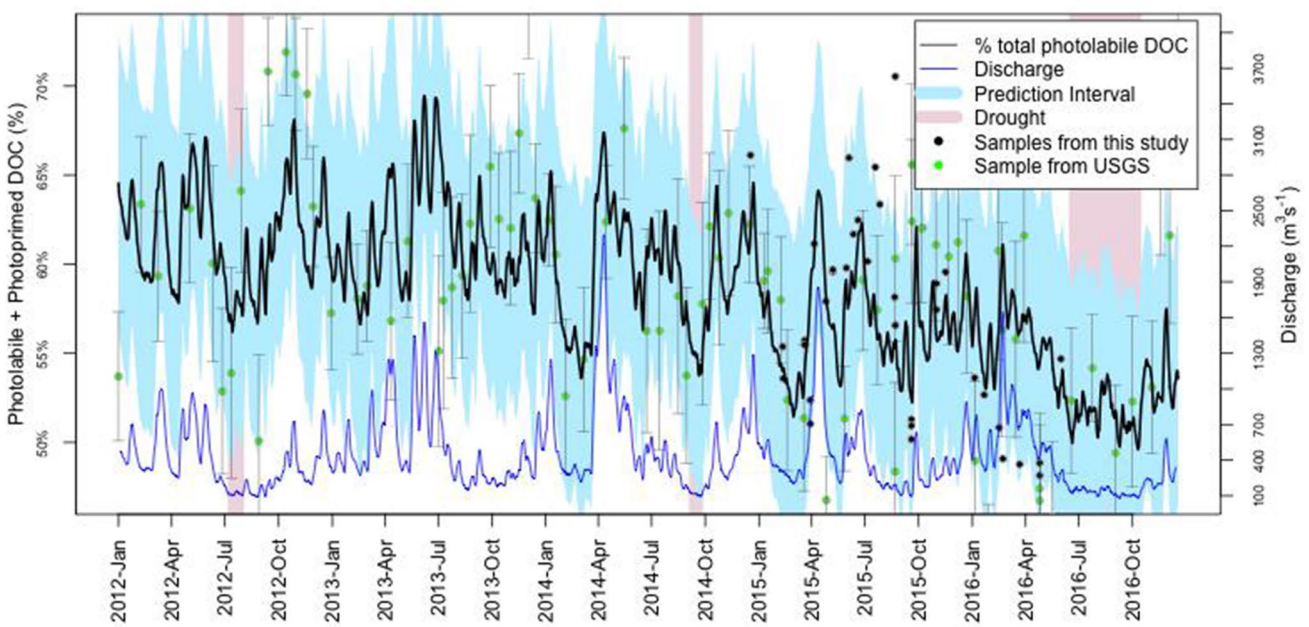

Fig. 6 Predicted daily percentage total photolability of dissolved organic carbon (DOC) exported from the Connecticut River. The total photolability of DOC is the sum of directly photolabile DOC and photoprimed biolabile DOC concentrations normalized by the initial total DOC concentration. Blue and red ribbons respectively show prediction interval and drought periods (0–10th percentile of 10-year discharge record). The prediction interval reflects both the bootstrap confidence intervals (95%) of the total photolabile model and the prediction intervals (95%) from the LOADEST. Total photolability and discharge are shown as 7-day rolling averages. The black circles represent photolability values that were directly measured during the study whereas the green circles represent photolability for USGS samples which were calculated from UV-absorbance and DOC concentration. The error bars on the USGS samples represent 95% confidence interval from the total photolabile DOC concentration model from this study (Supplementary Results S1)

Discussion

Our study examined the variability of biolability, photolability, and photoprimed biolability across large spatiotemporal and hydrological scales that are highly relevant to ecosystem science (Stanley et al. 2012; Creed et al. 2015; Raymond et al. 2016). The result is an expansive overview of what environmental variables correlate with lability across the Connecticut River watershed, and a clear depiction of how hydrological events facilitate the export of largely photolabile DOC fluxes across the riverine network (Fig. 6). Furthermore, the broad ranges of DOC quantity and quality presented in our study, which have not been tested for lability in a single experimentally uniform study to date (Supplementary Table S4), make our findings relevant for other ecosystems beyond our study watershed. The results of photolability and photpriming experiments, in particular, provide a new scalable method that estimates the flux of DOC that can be mineralized by sunlight and microbes upon export. This novel method showcases how a commonly measured parameter (a254) can be used for estimating the seasonal and annual fluctuations in photolabile DOC fluxes (Fig. 6, Supplementary Fig. 9), and also how to utilize existing database to assess the photolabile DOC fluxes of the past.

Biolability

The biolability values reported in our study span one of the largest ranges reported to date (Supplementary Table S4). In particular, some of the high biolability values observed in this study (> 50%; n = 11 out of 461) exceed values from past studies that involved longer incubation periods (51% over 898-days, Vähätalo and Wetzel 2008). While comparing results of lability experiments under different designs is not advisable, reporting of such high biolability warrants a careful examination and survey of the literature. First, it is worth noting that all biolability values above 50% in the present study were observed in samples collected during initial pulses of hydrological events that have previously been associated with enhanced bioavailability such as spring snowmelt (Holmes et al. 2008) or rain after fall leaf senescence (Sleighter et al. 2014; Singh et al. 2014). Initial pulses of DOC during storm events are often associated with increased biolability (Kaplan and Newbold 1995; Buffam and Galloway 2001; McLaughlin and Kaplan 2013) possibly due to highly biolabile nature of fresh organic matter in the upper soil layer (Butman et al. 2007) and leaf litter (McDowell 1985; Bernhardt and McDowell 2008; Caillon and Schelker 2020). Secondly, the nutrient amendment applied in our study may have boosted the microbial degradation of DOC samples that were collected during storms. Microbial degradation of DOC leached from soil or leaf litter can be limited by nutrient availability (Baldwin 1999; Marschner and Kalbitz 2003). Thus, we are confident that these highly biolabile samples are end-members of the biolability spectrum that resulted from the nature of event-driven DOC pulses, nutrient amendment, and expansive sampling, all of which were intended components of our study design.

Changes in CDOM absorbance during bioassays showed both decreases and increases, indicating that CDOM could be both reduced or increased by microbes. The overwhelming direction of change, however, was towards microbial utilization of CDOM, where more than 95% and 90% of the incubations showed decreases in a254 and a412, respectively. The directions of $S_{275\text{-}295}$, $S_{350\text{-}400}$, and S_R changes indicated flattening of the slope at the lower wavelengths and steepening in the higher wavelengths, as previously reported for biodegradation of CDOM (Helms et al. 2008). A slight increase in SUVA (1.7%) after biodegradation and the inverse relationship observed between SUVA and biolability (Fig. 4a) also conform to the notion that microbes preferentially degrade less aromatic DOC (Wickland et al. 2012; Koehler et al. 2012; Fellman et al. 2014; Frey et al. 2016; Hansen et al. 2016). However, it should be noted that changes in both $S_{275\text{-}295}$ and SUVA from biodegradation was not significant (Welch's t-test p-value > 0.05), which demonstrates that the microbial processing of biolabile DOC may not have a consistent effect on the spectral shape of CDOM. Furthermore, changes in $S_{275\text{-}295}$ and SUVA among highly biolabile samples (biolability > 30%; n = 36) were also statistically insignificant (Welch's *t* test p value > 0.1). In other words, the biological degradation of DOM during the bioassays consistently reduced the amount of CDOM but have little effect on the overall spectral shape of the CDOM. We postulate the diversity of DOM sources represented across our samples and relatively short duration of the bioassay may have led to the minor change in spectral shape observed in our study.

Photolability

Our results underscore the photolabile nature of riverine DOC. The linear regression between bulk DOC concentration and photolabile DOC concentration indicates that photolabile DOC constitutes more than a half of the total DOC pool across a wide range of samples (Fig. 3). This is presumably because allochthonous DOC from surrounding land is the dominant source of DOC in rivers, and that the chromophoric nature of the allochthonous DOC makes it susceptible to photomineralization (Stubbins et al. 2010; Benner and Kaiser 2011; Lapierre et al. 2013). The strong correlation observed between photolabile DOC concentration and a254 and a412, and also the inverse relationship between S_R and photolability in our study attest to the previously described

central role of aromatic CDOM in photochemical DOC reactions (Stubbins et al. 2008).

Photolability, measured in both concentration and percentage, was not correlated with watershed size or area-normalized discharge. Further, land cover characteristics showed statistically insignificant correlations with the proportion of photolabile DOC. This is contrary to past studies that showed landscape control of DOC quality. For example, changes in the optical properties (e.g. fluorescence index) have been linked to agricultural and wetland land cover (Wilson and Xeopolulous 2008), and the proportion of urban land cover within watersheds has been linked to lower photolability, higher biolability, changes in fluorescence, and older carbon age (Butman et al. 2012; Lu et al. 2013; Hosen et al. 2014; Williams et al. 2016). The lack of significant correlation by spatial factors in this study, however, does not imply that DOC quality in the Connecticut River watershed is not controlled by watershed geology and land cover, or that the landscape control of DOC quality is diminished in large watersheds. Our study design aimed to capture the diversity of DOC quality across different watersheds and hydrological conditions, rather than to collect representative samples that can help discern the importance of static spatial variable such as watershed size or land cover. Variation in hydrological conditions (Supplementary Fig. S2) are known to cause major shifts in DOC chemistry and lability (Fellman et al. 2009; Wilson et al. 2013; Spencer et al. 2015; Wagner et al. 2019) and are predicted to create more homogeneous DOC quality at higher flows across a large watershed due to the shunting of terrestrial DOC downstream (Raymond et al. 2016, Hosen et al. 2020). Thus, sampling baseflow and storm events in this study may have masked the correlation with landscape variables that could otherwise be more significant when sampling only at baseflow conditions. Further, it should be noted that the selection of watersheds in this study included a narrow range of non-forest land covers (Supplementary Table S1) and we did not examine the importance of land cover across different watershed sizes. Future studies should be designed with consideration for capturing wide ranges of both dynamic and static controls of DOC in order to discern when and where static variables have greater control.

Coupled biological and photochemical processing of DOC

Our study showcases the prevalence of photoprimable DOC in riverine systems. Despite the long history of studies on the effect of photoreactions for biological DOC utilization, only few published studies examined photopriming across large spatial scales and over different flow regimes (Stepanauskas et al. 2005; Cory et al. 2014), and most studies focused on smaller watersheds or specific transport pathways within the aquatic carbon cycle (e.g. lakes, leaf matter, cyanobacteria; Tranvik and Kokalji 1998; Tranvik and Bertilsson 2001; Fasching and Battin 2012; Fellman et al. 2013; Bittar et al. 2015). Covering large spatiotemporal and hydrological gradients, the samples in our study showed that the amount of photoprimed biolabile DOC was often greater than the initial biolabile DOC despite the sizable removal of DOC during 30-day irradiations. On average, the release of additional biolabile DOC by photopriming tripled the amount of total bioavailable DOC (i.e. biolabile DOC + photoprimed biolabile DOC). In other words, the release of biolabile DOC through photopriming had greater impact on the net removal of riverine DOC than the microbial uptake with DOC in the dark. However, our estimate should be considered as a potential range of photopriming at longer time scale (i.e. near-complete removal of CDOM) rather than a comparison to past studies with different research designs (e.g. light exposure, nutrient amendment, incubation duration) or in-situ photopriming rate.

Biological degradation of DOC changed CDOM absorbance among samples. Yet, the relationship between the remaining CDOM (a254) and photolabile DOC concentration was largely unaffected. In other words, the changes in DOC composition by microbes did not have a large effect on the robustness of using a254 as a predictor for concentration of photolabile DOC (Supplementary Fig. S6; Supplementary Result S1), suggesting that biological processing of DOC does not affect the inherent relationship between short wavelength absorbance and photolability. This implies that the photolabile DOC model presented here can be used regardless of biodegradation history of DOC, which makes it more robust and potentially more applicable to other systems.

Predicting photolabile DOC with CDOM

The strong correlations found between CDOM (a254 and a412) and the concentrations of photolabile and total photolabile DOC (photomineralized + photoprimed) provide a potentially important tool for constraining the amount of photolabile DOC exported from temperate rivers (Fig. 4B, Supplementary Fig. S5B). The independent variables of the models reflect that the light-absorbing aromatic CDOM is the main source of photomineralization. Our results build upon past studies that presented strong correlations between photolabile DOC loss and UV absorbance at various wavelengths (Bertilsson and Tranvik 2000; Helms et al. 2014; Koehler et al. 2016). Further, the models presented here are in agreement with a recent study that showed a robust relationship between photomineralization and photobleaching across 10 global rivers (Aarnos et al. 2018). Whereas the work by Aarnos and colleagues modeled photomineralization with photobleaching, our models are based on the

CDOM absorbance, which was almost completely bleached during the incubations.

The model for total photolabile DOC concentration and the residual analysis of the photolabile DOC model (Fig. 5B; Supplementary Fig. S7) present a novel insight on photochemical DOC modification. The ratio between the photoprimed biolabile DOC and photolabile DOC effectively explained the residual of the a254 photolabile DOC model ($r^2 = 0.46$, Supplementary Fig. S6B). This indicates that the deviation from the regression is a manifestation of partially photodegraded molecules that were not photolabile under our experimental conditions but are highly biolabile. Further, the sum of photolabile and photoprimed biolabile DOC showed a stronger correlation with both a254 and a412 in comparison to the regression model built with only photolabile DOC (Fig. 5; Supplementary Figure S5; Supplementary Result S1). This implies that the DOC UV absorbance is a better indicator for total photolabile DOC than just photomineralization because the quality of DOC causes variable ratios of DOC to be completely photomineralized versus photoprimed. In addition, applying the total photolabile DOC concentration model (Figure S5B; Supplementary Result S1) may depict a more appropriate theoretical limit for photochemical DOC removal in natural settings where both photomineralization and microbial respiration of photoprimed biolabile DOC occur concurrently. Furthermore, the stronger correlation of the total photolabile DOC model can help reduce the margin of error for estimating the outcomes of photochemical processes at large spatiotemporal scales (Supplementary Result S1).

The robustness of the photolabile DOC model with a412 (Supplementary Fig. S4) extends the scalability of our findings since a412 can be retrieved from SeaWiFS and MODIS satellites (Tehrani et al. 2013). Now, in conjunction with predicting hydrophobic organic acid fraction and aromaticity (Weishaar et al. 2003; Spencer et al. 2012), a254 and a412 can be used for estimating the concentrations and export of photolabile DOC. This is a potentially important tool, as it is currently not possible to accurately model the light environment or DOC quantum yields accurately over a large watershed in order to have a more process-based estimation of photochemical DOC removal.

Photolabile DOC export from the Connecticut River

LOADEST model estimates for the Connecticut River reveal that a large fraction of the DOC export to Long Island Sound is photolabile and photoprimable (Fig. 6, Supplementary Fig. S9), and points to inefficient photodegradation during transport. Light is intercepted by tree canopies in small forested watersheds, and riverine turbidity and CDOM can severely limit light penetration (Juday and Birge 1933) regardless of land cover. The limited nature of DOC-sunlight interactions in our fluvial samples is also indirectly demonstrated in our reservoir samples that have very low UV absorbance and photolability (Figs. 3, 4, 5), presumably due to long residence times and light regimes that facilitate greater photochemical degradation than in rivers (Köhler et al. 2013; Vähätalo and Wetzel 2008). At the watershed scale, however, the DOC flux leaving the Connecticut River is still highly photolabile despite the 15,000 lakes, ponds, and reservoirs in its watershed (USGS National Hydrography Dataset). Further, the majority of the DOC is exported during hydrologic events (Fig. 6; Supplementary Fig. S9; Raymond and Saiers 2010; Yoon and Raymond 2012), which are accompanied with high levels of turbidity and CDOM, and shorter reaction time for the transported DOC. In addition, an increase in cloud cover during rain events can also translate to less irradiance. In other words, photochemical reactions are severely limited and the residence time is shortened during the periods when the largest flux of photoreactive DOC is being transported. Thus, we argue that light availability during hydrologic events is a strong determinant for the amount and characteristics of DOC flux to the coastal ocean. This conclusion adds to past studies that suggested light availability as a key control for photomineralization in inland waters (Kirk 1994; Koehler et al. 2014).

Our study period captured multiple periods of drought conditions where water levels dropped to 50–70 year lows (Hosen et al. 2019). During these occasions, the total photolability of Connecticut River DOC fell below 50% (Fig. 6). The potential drivers of such low DOC photolability include the prevalence of groundwater with lower SUVA during base flow conditions, photochemical removal of DOC, and production of autochthonous DOC with low CDOM (Hosen et al. 2020). In contrast, DOC total photolability increased to upward of 70% during high discharge conditions such as spring snow melt and intense rain events (Fig. 6) when inputs of terrigenous DOC through surface and soil flowpaths typically dominate the hydrograph (Evans and Davies 1998) and residence times were shortest in the river network. Thus, DOC source and hydrology had a clear impact upon the quality of DOC exported from the river system, with low flow conditions exporting DOC with lower photolability and high discharge events exporting highly photolabile DOC, which supports the Pulse Shunt Concept proposed by Raymond et al. (2016). However, it should be noted that most DOC flux models, including LOADEST, tend to underestimate fluxes during storm events because samples capturing dynamic changes during events are underrepresented (Raymond and Saiers 2010; Yoon and Raymond 2012). In the case of modeling photolability or photolabile flux, the accuracy of the model depends on the availability of a254 measurements which can be obtained continuously in-situ with sensors. Thus, future studies should utilize data from submersible sensors in conjunction with grab samples to

improve the accuracy and spatiotemporal resolution of their models.

Role of photochemical processing for terrestrial DOC

The critical role of photolabile DOC in inland rivers has been identified in other large rivers. In the Congo River where the water residence time has a strong seasonality, photochemical DOC degradation and its byproduction of lower molecular weight derivatives have been identified as the key determinants of DOC quality along the downstream transport (Lambert et al. 2016). Similarly, continuous supply of biolabile DOC through photopriming has been pointed as a possible mechanism behind the steady biolability of DOC along the Kolyma River in the arctic (Frey et al. 2016). Yet, DOC export from large riverine systems such as the Congo, Amazon, or Mississippi remain photolabile upon entering their respective coastal zones (Spencer et al. 2009; Medeiros et al. 2015; Lambert et al. 2016).

High levels of photolabile DOC exported from freshwater networks imply that photopriming may play a key role in facilitating more rapid degradation of terrestrial DOC in coastal margins (Miller and Zepp 1995, Moran and Zepp 1997; Aarnos et al. 2018). As dilution with seawater and settling of sediment releases the light limitation, terrigenous DOC from large rivers encounters improved conditions for photochemical DOC removal and photopriming in coastal margins. In the case of the Louisiana Shelf, to which the Mississippi River drains, this process of photochemical transformation is estimated to enhance the biological DOC removal by 50% (Fichot and Benner 2014). For the Amazon River plume in the Atlantic Ocean, photochemical transformation was a key factor in explaining spatial and seasonal variations of the terrigenous DOC quality as it became diluted with seawater (Medeiros et al. 2015). At global scale, roughly a third of riverine DOC flux into the ocean is estimated to be removed through photomineralization and photopriming within 1 year (Aarnos et al. 2018). Results from our study add to these previous studies, and emphasize the critical role of photochemical processes and highlight the importance of hydrologic events as a strong driver of both the quantity and quality of DOC exported from riverine networks.

Conclusion

Understanding potential flux of photolabile and photoprimable DOC from riverine systems is a crucial part of studying the carbon linkage between terrestrial and marine systems. The net mineralization through these two removal pathways, in conjunction with biomineralization, has a large impact on the metabolic status of waterbodies and their CO_2 fluxes into the atmosphere (Prairie 2008; Cory et al. 2014). Yet, the variability of photolability and the effect of photopriming at large spatiotemporal scales is poorly understood, especially in the context of event-driven DOC pulses that control the DOC export from inland waters (Raymond et al. 2016). This study presents a range of photochemical and photoprimed biolability encountered across a large number of samples that captures the diverse land use, hydrological, and seasonal conditions within the Connecticut River. By relating photolabile DOC to a254 and a412, this study presents a convenient method for estimating the amount of total photolabile DOC in a river water sample from either simple spectrophotometric measurements or remote sensing data. The correlation reported may be broadly applicable to temperate New England, and even globally, although future experiments under similar conditions would strengthen this assumption. The amount of photolabile DOC that escapes the Connecticut River and its variation across seasons also suggest that the dominant control on DOC transport by hydrological events (Raymond et al. 2016) extends to both quantity and quality of DOC in inland waters.

Acknowledgement We would like to thank the USGS and the Metropolitan District for granting access to their sites and assisting us in sampling for this study. Any use of trade, firm, or product name is for descriptive purposes only and does not imply endorsement by the U.S. Government. This project was funded by NSF Awards 1601155, 1340749, and 1267645.

Compliance with ethical standards

Conflict of interest The authors declare that they have no competing interest.

References

Aarnos H, Gélinas Y, Kasurinen V et al (2018) Photochemical mineralization of terrigenous DOC to dissolved inorganic carbon in ocean. Global Biogeochem Cycles 32:250–266. https://doi.org/10.1002/2017GB005698

Baldwin DS (1999) Dissolved organic matter and phosphorus leached from fresh and terrestrially aged river red gum leaves : implications for assessing river floodplain interactions. Freshwater 41:675–685

Benda L, Dunne T (1997) Stochastic forcing of sediment routing and storage in channel networks. Water Resour Res 33:2865–2880

Benner R, Kaiser K (2011) Biological and photochemical transformations of amino acids and lignin phenols in riverine dissolved organic matter. Biogeochemistry 102:209–222. https://doi.org/10.1007/s10533-010-9435-4

Berggren M, Laudon H, Haei M et al (2010) Efficient aquatic bacterial metabolism of dissolved low-molecular-weight compounds from terrestrial sources. ISME J 4:408–416. https://doi.org/10.1038/ismej.2009.120

Bernhardt ES, McDowell WH (2008) Twenty years apart: comparisons of DOM uptake during leaf leachate releases to Hubbard Brook

Valley streams in 1979 versus 2000. J Geophys Res 113:1–8. https://doi.org/10.1029/2007JG000618
Bertilsson S, Tranvik LJ (2000) Photochemical transformation of dissolved organic matter in lakes. Limnol Oceanogr 45:753–762. https://doi.org/10.4319/lo.2000.45.4.0753
Bittar TB, Vieira AAH, Stubbins A, Mopper K (2015) Competition between photochemical and biological degradation of dissolved organic matter from the cyanobacteria microcystis aeruginosa. Limnol Oceanogr 60:1172–1194. https://doi.org/10.1002/lno.10090
Buffam I, Galloway J (2001) A stormflow/baseflow comparison of dissolved organic matter concentrations and bioavailability in an Appalachian stream. Biogeochemistry 53:269–306
Butman D, Raymond P, Oh N, Mull K (2007) Quantity, C age and lability of desorbed soil organic carbon in fresh water and seawater. Org Geochem 38:1547–1557. https://doi.org/10.1016/j.orggeochem.2007.05.011
Butman D, Raymond PA, Butler K, Aiken G (2012) Relationships between Δ 14 C and the molecular quality of dissolved organic carbon in rivers draining to the coast from the conterminous United States. Global Biogeochem Cycles. https://doi.org/10.1029/2012GB004361
Cai W (2011) Estuarine and coastal ocean carbon paradox : CO2 sinks or sites of terrestrial carbon incineration ? Ann Rev Mar Sci 3:123–145. https://doi.org/10.1146/annurev-marine-120709-142723
Caillon F, Schelker J (2020) Dynamic transfer of soil bacteria and dissolved organic carbon into small streams during hydrological events. Aquat Sci 82:1–11. https://doi.org/10.1007/s00027-020-0714-4
Canty A, Ripley B (2020) Boot: Bootstrap R (S-Plus) Functions. R package version 1.3–25.
Caplanne S, Laurion I (2008) Effect of chromophoric dissolved organic matter on epilimnetic stratification in lakes. Aquat Sci 70:123–133. https://doi.org/10.1007/s00027-007-7006-0
Carpenter SR, Cole JJ, Kitchell JF, Pace ML (1998) Impact of dissolved organic carbon, phosphorus, and grazing on phytoplankton biomass and production in experimental lakes. Limnol Oceanogr 43:73–80. https://doi.org/10.4319/lo.1998.43.1.0073
Catalán N, Marcé R, Kothawala DN, Tranvik LJ (2016) Organic carbon decomposition rates controlled by water retention time across inland waters. Nat Geosci 9:1–7. https://doi.org/10.1038/ngeo2720
Christman RF, Norwood DL, Millington DS et al (1983) Identity and yields of major halogenated products of aquatic fulvic acid chlorination. Environ Sci Technol 17:625–628. https://doi.org/10.1021/es00116a012
Cory RM, Kling GW (2018) Interactions between sunlight and microorganisms influence dissolved organic matter degradation along the aquatic continuum. Limnol Oceanogr Lett. https://doi.org/10.1002/lol2.10060
Cory RM, Ward CP, Crump BC, Kling GW (2014) Sunlight controls water column processing of carbon in arctic fresh waters. Science 345(80):925–928. https://doi.org/10.1126/science.1253119
Creed IF, McKnight DM, Pellerin BA et al (2015) The river as a chemostat: Fresh perspectives on dissolved organic matter flowing down the river continuum. Can J Fish Aquat Sci 72:1272–1285. https://doi.org/10.1139/cjfas-2014-0400
Davison AC, Hinkley DV (1997) Bootstrap methods and their applications. Cambridge University Press, Cambridge (**ISBN 0-521-57391-2**)
Downing BD, Pellerin BA, Bergamaschi BA et al (2012) Seeing the light: the effects of particles, dissolved materials, and temperature on in situ measurements of DOM fluorescence in rivers and streams. Limnol Ocean Methods 10:767–775. https://doi.org/10.4319/lom.2012.10.767
EPA National Hydrography Dataset Plus Version 2. http://www.horizon-systems.com/NHDPlus/NHDPlusV2_home.php. Accessed 9 Nov 2019
Erlandsson M, Cory N, Köhler S, Bishop K (2010) Direct and indirect effects of increasing dissolved organic carbon levels on pH in lakes recovering from acidification. J Geophys Res 115:G03004. https://doi.org/10.1029/2009JG001082
Evans C, Davies TD (1998) RESOURCES Causes of concentration/discharge hysteresis and its potential as a tool for analysis of episode hydrochemistry. Water Resour Res 34:129–137
Fasching C, Battin TJ (2012) Exposure of dissolved organic matter to UV-radiation increases bacterial growth efficiency in a clear-water Alpine stream and its adjacent groundwater. Aquat Sci 74:143–153. https://doi.org/10.1007/s00027-011-0205-8
Fellman JB, Hood E, D'Amore DV et al (2009) Seasonal changes in the chemical quality and biodegradability of dissolved organic matter exported from soils to streams in coastal temperate rainforest watersheds. Biogeochemistry 95:277–293. https://doi.org/10.1007/s10533-009-9336-6
Fellman JB, Petrone KC, Grierson PF (2013) Leaf litter age, chemical quality, and photodegradation control the fate of leachate dissolved organic matter in a dryland river. J Arid Environ 89:30–37. https://doi.org/10.1016/j.jaridenv.2012.10.011
Fellman JB, Spencer RGM, Raymond PA, et al (2014) Dissolved organic carbon biolability decreases along with its modernization in fluvial networks in an ancient landscape. Ecology 95:2622–2632. https://doi.org/10.1890/13-1360.1
Fichot CG, Benner R (2014) The fate of terrigenous dissolved organic carbon in a river-influenced ocean margin. Global Biogeochem Cycles 28:300–318. https://doi.org/10.1002/2013GB004670
Fisher SG, Likens GE (1973) Energy flow in bear brook, new hampshire : an integrative approach to stream. Ecol Monogr 43:421–439
Frey KE, Sobczak WV, Mann PJ, Holmes RM (2016) Optical properties and bioavailability of dissolved organic matter along a flow-path continuum from soil pore waters to the Kolyma River mainstem, East Siberia. Biogeosciences 13:2279–2290. https://doi.org/10.5194/bg-13-2279-2016
Gueymard CA (2001) Parameterized transmittance model for direct beam and circumsolar spectral irradiance. Sol Energy 71:325–346. https://doi.org/10.1016/S0038-092X(01)00054-8
Hansen AM, Kraus TEC, Pellerin BA et al (2016) Optical properties of dissolved organic matter (DOM): effects of biological and photolytic degradation. Limnol Oceanogr 61:1015–1032. https://doi.org/10.1002/lno.10270
Helms JR, Mao J, Stubbins A et al (2014) Loss of optical and molecular indicators of terrigenous dissolved organic matter during long-term photobleaching. Aquat Sci 76:353–373. https://doi.org/10.1007/s00027-014-0340-0
Helms JR, Stubbins A, Ritchie JD et al (2008) Absorption spectral slopes and slope ratios as indicators of molecular weight, source, and photobleaching of chromophoric dissolved organic matter. Limnol Oceanogr 53:955–969. https://doi.org/10.4319/lo.2008.53.3.0955
Holmes RM, McClelland JW, Raymond PA et al (2008) Lability of DOC transported by Alaskan rivers to the Arctic Ocean. Geophys Res Lett 35:3–7. https://doi.org/10.1029/2007GL032837
Homer CG, Dewitz JA, Yang L, et al (2015) Completion of the 2011 National Land Cover Database for the conterminous United States-Representing a decade of land cover change information. Photogramm Eng Remote Sensing 81:345–354. https://doi.org/10.14358/PERS.81.5.345
Hosen JD, Aho KS, Appling AP et al (2019) Enhancement of primary production during drought in a temperate watershed is greater in larger rivers than headwater streams. Limnol Oceanogr 64:1–15. https://doi.org/10.1002/lno.11127

Hosen JD, Aho KS, Fair JH et al (2020) Source switching maintains dissolved organic matter chemostasis across discharge levels in a large temperate river network. Ecosystems. https://doi.org/10.1007/s10021-020-00514-7

Hosen JD, McDonough OT, Febria CM, Palmer MA (2014) Dissolved organic matter quality and bioavailability changes across an urbanization gradient in headwater streams. Environ Sci Technol 48:7817–7824. https://doi.org/10.1021/es501422z

Hotchkiss ER Jr, ROH, Sponseller RA, et al (2015) Sources of and processes controlling CO_2 emissions change with the size of streams and rivers. Nat Geosci. https://doi.org/10.1038/NGEO2507

Jennings E, Jones S, Arvola L et al (2012) Effects of weather-related episodic events in lakes: an analysis based on high-frequency data. Freshw Biol 57:589–601. https://doi.org/10.1111/j.1365-2427.2011.02729.x

Juday C, Birge EA (1933) The transparency, the color and the specific conductance of the lake waters of northeastern Wisconsin. Trans Wis Acad Sci Arts Lett 28:205–259

Judd KE, Crump BC, Kling GW (2006) Variation in dissolved organic matter controls bacterial production and community composition Tl-87. Ecology 87:2068–2079. https://doi.org/10.1890/0012-9658(2006)87[2068:VIDOMC]2.0.CO;2

Junk WJ, Bayley PB, Sparks RE (1989) The flood pulse concept in river-floodplain systems. Proc Int Large River Symp Can Spec Publ Fish Aquat Sci 106:110–127. https://doi.org/10.1371/journal.pone.0028909

Kaplan LA, Newbold JD (1995) Measurement of streamwater biodegradable dissolved organic carbon with a plug-flow bioreactor. Water Res 29:2696–2706. https://doi.org/10.1016/0043-1354(95)00135-8

Kirchman D, Dittel A, Findlay S, Fischer D (2004) Changes in bacterial activity and community structure in response to dissolved organic matter in the Hudson River, New York. Aquat Microb 35:243–257

Kirk JTO (1994) Light and photosynthesis in aquatic ecosystems. 2nd edition, xvi, 509p. Cambridge University Press, 1994. J Mar Biol Assoc UK 74:987. https://doi.org/10.1017/S0025315400044180

Kitis M, Kilduff JE, Karanfil T (2001) Isolation of dissolved organic matter (dom) from surface waters using reverse osmosis and its impact on the reactivity of dom to formation and speciation of disinfection by-products. Water Res 35:2225–2234. https://doi.org/10.1016/S0043-1354(00)00509-1

Koehler B, Broman E, Tranvik LJ (2016) Apparent quantum yield of photochemical dissolved organic carbon mineralization in lakes. Limnol Oceanogr 61:2207–2221. https://doi.org/10.1002/lno.10366

Koehler B, Landelius T, Weyhenmeyer GA et al (2014) Sunlight-induced carbon dioxide emissions from inland waters. Global Biogeochem Cycles 28:927–949. https://doi.org/10.1002/2014GB004853

Koehler B, von Wachenfeldt E, Kothawala D, Tranvik LJ (2012) Reactivity continuum of dissolved organic carbon decomposition in lake water. J Geophys Res 117:G01024. https://doi.org/10.1029/2011JG001793

Köhler SJ, Kothawala D, Futter MN et al (2013) In-lake processes offset increased terrestrial inputs of dissolved organic carbon and color to lakes. PLoS One 8:1–12. https://doi.org/10.1371/journal.pone.0070598

Lambert T, Bouillon S, Darchambeau F et al (2016) Shift in the chemical composition of dissolved organic matter in the Congo River network. Biogeosciences 13:5405–5420. https://doi.org/10.5194/bg-13-5405-2016

Lapierre JF, Del Giorgio PA (2014) Partial coupling and differential regulation of biologically and photochemically labile dissolved organic carbon across boreal aquatic networks. Biogeosciences 11:5969–5985. https://doi.org/10.5194/bg-11-5969-2014

Lapierre J-F, Guillemette F, Berggren M, Del Giorgio PA (2013) Increases in terrestrially derived carbon stimulate organic carbon processing and CO_2 emissions in boreal aquatic ecosystems. Nat Commun 4:2972. https://doi.org/10.1038/ncomms3972

Lindell MJ, Granéli W, Tranvik LJ (1995) Enhanced bacterial growth in response to photochemical transformation of dissolved organic matter. Limnol Oceanogr 40:195–199. https://doi.org/10.4319/lo.1995.40.1.0195

Lu Y, Bauer JE, Canuel EA et al (2013) Photochemical and microbial alteration of dissolved organic matter in temperate headwater streams associated with different land use. J Geophys Res Biogeosci 118:566–580. https://doi.org/10.1002/jgrg.20048

Mann PJ, Sobczak WV, Larue MM et al (2014) Evidence for key enzymatic controls on metabolism of Arctic river organic matter. Glob Chang Biol 20:1089–1100. https://doi.org/10.1111/gcb.12416

Marschner B, Kalbitz K (2003) Controls of bioavailability and biodegradability of dissolved organic matter in soils. In: Geoderma. pp 211–235

McDowell WHM (1985) Kinetics and mechanisms of dissolved organic carbon retention in a headwater stream. Biogeochemistry 1:329–352. https://doi.org/10.1007/BF02187376

McDowell W, Likens G (1988) Origin, composition, and flux of dissolved organic carbon in the Hubbard Brook Valley. Ecol Monogr 58:177–195

McDowell WH, Zsolnay A, Aitkenhead-Peterson JA et al (2006) A comparison of methods to determine the biodegradable dissolved organic carbon from different terrestrial sources. Soil Biol Biochem 38:1933–1942. https://doi.org/10.1016/j.soilbio.2005.12.018

McLaughlin C, Kaplan LA (2013) Biological lability of dissolved organic carbon in stream water and contributing terrestrial sources. Freshw Sci 32:1219–1230. https://doi.org/10.1899/12-202.1

Medeiros P, Seidel M, Ward ND et al (2015) Fate of the Amazon River dissolved organic matter in the tropical Atlantic Ocean. Global Biogeochem Cycles. https://doi.org/10.1002/2015GB005115.Received

Miller WL, Zepp RG (1995) Photochemical production of dissolved inorganic carbon from terrestrial organic matter: significance to the oceanic organic carbon cycle. Geophys Res Lett 22:417–420. https://doi.org/10.1029/94GL03344

Mopper K, Zhou X, Kieber RJ et al (1991) Photochemical degradation of dissolved organic carbon and its impact on the oceanic carbon cycle. Nature 353:60–62

Mopper K, Kieber DJ, Stubbins A (2015) Marine photochemistry of organic matter: processes and impacts. Processes and Impacts.

Moran MA, Zepp RG (1997) Role of photoreactions in the formation of biologically labile compounds from dissolved organic matter. Limnol Oceanogr 42:1307–1316

Osburn CL, Retamal L, Vincent WF (2009) Photoreactivity of chromophoric dissolved organic matter transported by the Mackenzie River to the Beaufort Sea. Mar Chem 115:10–20. https://doi.org/10.1016/j.marchem.2009.05.003

Pellerin BA, Saraceno JF, Shanley JB et al (2012) Taking the pulse of snowmelt: in situ sensors reveal seasonal, event and diurnal patterns of nitrate and dissolved organic matter variability in an upland forest stream. Biogeochemistry 108:183–198. https://doi.org/10.1007/s10533-011-9589-8

Prairie YT (2008) Carbocentric limnology: looking back, looking forward. Can J Fish Aquat Sci 65:543–548. https://doi.org/10.1139/f08-011

R Core Team (2013) R: A language and environment for statistical computing. R Foundation for Statistical Computing, Vienna, Austria. http://www.R-project.org/

Raymond PA, Hartmann J, Lauerwald R et al (2013) Global carbon dioxide emissions from inland waters. Nature 503:355–9. https://doi.org/10.1038/nature12760

Raymond PA, Saiers JE (2010) Event controlled DOC export from forested watersheds. Biogeochemistry 100:197–209. https://doi.org/10.1007/s10533-010-9416-7

Raymond PA, Saiers JE, Sobczak WV (2016) Hydrological and biogeochemical controls on watershed dissolved organic matter transport: pulse-shunt concept. Ecology 97:5–16. https://doi.org/10.1890/14-1684.1

Redfield AC (1934) On the proportions of organic derivatives in sea water and their relation to the composition of plankton. James Jonstone Memorial. Liverpool University Press, Liverpool, pp 176–192

Runkel RL, Crawford CG, Cohn TA (2004) Load Estimator (LOADEST): A FORTRAN program for estimating constituent loads in streams and rivers. U.S. Geological Survey

Sayama T, McDonnell JJ (2009) A new time-space accounting scheme to predict stream water residence time and hydrograph source components at the watershed scale. Water Resour Res 45:1–14. https://doi.org/10.1029/2008WR007549

Shultz M, Pellerin B, Aiken G et al (2018) High frequency data exposes nonlinear seasonal controls on dissolved organic matter in a large watershed. Environ Sci Technol 52:5644–5652. https://doi.org/10.1021/acs.est.7b04579

Singh S, Inamdar S, Mitchell M, McHale P (2014) Seasonal pattern of dissolved organic matter (DOM) in watershed sources: influence of hydrologic flow paths and autumn leaf fall. Biogeochemistry 118:321–337. https://doi.org/10.1007/s10533-013-9934-1

Sleighter RL, Cory RM, Kaplan LA et al (2014) A coupled geochemical and biogeochemical approach to characterize the bioreactivity of dissolved organic matter from a headwater stream. J Geophys Res Biogeosciences. https://doi.org/10.1002/2013JG002600.Received

Spencer RGM, Butler KD, Aiken GR (2012) Dissolved organic carbon and chromophoric dissolved organic matter properties of rivers in the USA. J Geophys Res Biogeosci. https://doi.org/10.1029/2011JG001928

Spencer RGM, Mann PJ, Dittmar T et al (2015) Detecting the signature of permafrost thaw in Arctic rivers. Geophys Res Lett 42:2830–2835. https://doi.org/10.1002/2015GL063498

Spencer RGM, Stubbins A, Hernes PJ et al (2009) Photochemical degradation of dissolved organic matter and dissolved lignin phenols from the Congo River. J Geophys Res Biogeosci 114:1–12. https://doi.org/10.1029/2009JG000968

Stanley EH, Powers SM, Lottig NR et al (2012) Contemporary changes in dissolved organic carbon (DOC) in human-dominated rivers: is there a role for DOC management? Freshw Biol 57:26–42. https://doi.org/10.1111/j.1365-2427.2011.02613.x

Stepanauskas R, Moran MA, Bergamaschi BA, Hollibaugh JT (2005) Sources, bioavailability, and photoreactivity of dissolved organic carbon in the Sacramento-San Joaquin River Delta. Biogeochemistry 74:131–149. https://doi.org/10.1007/s10533-004-3361-2

Strome DJ, Miller MC (1978) Photolytic changes in dissolved humic substances. SIL Proceedings 1922–2010(20):1248–1254. https://doi.org/10.1080/03680770.1977.11896681

Stubbins A, Hubbard V, Uher G et al (2008) Relating carbon monoxide photoproduction to dissolved organic matter functionality. Environ Sci Technol 42:3271–3276. https://doi.org/10.1021/es703014q

Stubbins A, Mann PJ, Powers L et al (2017) Low photolability of yedoma permafrost dissolved organic carbon. J Geophys Res Biogeosci 122:200–211. https://doi.org/10.1002/2016JG003688

Stubbins A, Spencer RGM, Chen H et al (2010) Illuminated darkness: molecular signatures of Congo River dissolved organic matter and its photochemical alteration as revealed by ultrahigh precision mass spectrometry. Limnol Oceanogr 55:1467–1477. https://doi.org/10.4319/lo.2010.55.4.1467

Tehrani NC, D'Sa EJ, Osburn CL et al (2013) Chromophoric dissolved organic matter and dissolved organic carbon from sea-viewing wide field-of-view sensor (seawifs), moderate resolution imaging spectroradiometer (modis) and meris sensors: case study for the northern gulf of mexico. Remote Sens 5:1439–1464. https://doi.org/10.3390/rs5031439

Thorp J, Delong M (1994) The riverine productivity model: an heuristic view of carbon sources and organic processing in large river ecosystems. Oikos 70:305–308

Tranvik LJ, Bertilsson S (2001) Contrasting effects of solar UV radiation on dissolved organic sources for bacterial growth. Ecol Lett 4:458–463. https://doi.org/10.1046/j.1461-0248.2001.00245.x

Tranvik L, Kokalj S (1998) Decreased biodegradability of algal DOC due to interactive effects of UV radiation and humic matter. Aquat Microb Ecol 14:301–307

Twardowski MS, Boss E, Sullivan JM, Donaghay PL (2004) Modeling the spectral shape of absorption by chromophoric dissolved organic matter. Mar Chem 89:69–88. https://doi.org/10.1016/j.marchem.2004.02.008

USGS Water Data for the Nation. https://waterdata.usgs.gov/nwis. Accessed 9 Nov 2019

USGS National Hydrgraphy Dataset. https://www.usgs.gov/core-science-systems/ngp/national-hydrography/national-hydrography-dataset?qt-science_support_page_related_con=0#qt-science_support_page_related_con. Accessed 9 Nov 2019

Vannote R, Minshall G, Cummins K et al (1980) The river continuum concept. Can J Fish Aquat Sci 37:130–137

Vidon P, Karwan DL, Andres AS et al (2018) In the path of the hurricane: impact of Hurricane Irene and Tropical Storm Lee on watershed hydrology and biogeochemistry from North Carolina to Maine, USA. Biogeochemistry. https://doi.org/10.1007/s10533-018-0423-4

Vähätalo AV, Wetzel RG (2008) Long-term photochemical and microbial decomposition of wetland-derived dissolved organic matter with alteration of 13C:12C mass ratio. Limnol Oceanogr 53:1387–1392. https://doi.org/10.4319/lo.2008.53.4.1387

Wagner S, Fair JH, Matt S et al (2019) Molecular Hysteresis : Hydrologically Driven Changes in Riverine Dissolved Organic Matter Chemistry During a Storm Event. JGR Biogeosciences 124:759–774. https://doi.org/10.1029/2018JG004817

Ward CP, Cory RM (2016) Complete and partial photo-oxidation of dissolved organic matter draining permafrost soils. Environ Sci Technol 50:3545–3553. https://doi.org/10.1021/acs.est.5b05354

Ward CP, Nalven SG, Crump BC et al (2017) Photochemical alteration of organic carbon draining permafrost soils shifts microbial metabolic pathways and stimulates respiration. Nat Commun 8:1–7. https://doi.org/10.1038/s41467-017-00759-2

Weishaar JL, Aiken GR, Bergamaschi BA et al (2003) Evaluation of specific ultraviolet absorbance as an indicator of the chemical composition and reactivity of dissolved organic carbon. Environ Sci Technol 37:4702–4708

Wickland KP, Aiken GR, Butler K et al (2012) Biodegradability of dissolved organic carbon in the Yukon River and its tributaries: Seasonality and importance of inorganic nitrogen. Global Biogeochem Cycles 26:1–14. https://doi.org/10.1029/2012GB004342

Williams CJ, Frost PC, Morales-Williams AM et al (2016) Human activities cause distinct dissolved organic matter composition across freshwater ecosystems. Glob Chang Biol 22:613–626. https://doi.org/10.1111/gcb.13094

Wilson HF, Saiers JE, Raymond PA, Sobczak WV (2013) Hydrologic drivers and seasonality of dissolved organic carbon concentration, nitrogen content, bioavailability, and export in a forested new England stream. Ecosystems 16:604–616. https://doi.org/10.1007/s10021-013-9635-6

Wilson HF, Xenopoulos MA (2008) Effects of agricultural land use on the composition of fluvial dissolved organic matter. Nat Geosci 2:37–41. https://doi.org/10.1038/ngeo391

Yoon B, Raymond PA (2012) Dissolved organic matter export from a forested watershed during Hurricane Irene. Geophys Res Lett 39:1–6. https://doi.org/10.1029/2012GL052785